LAWRENCE
LIVERMORE
NATIONAL
LABORATORY

Observation of a Kelvin-Helmholtz Instability in a High-Energy-Density Plasma on the Omega Laser

E. C. Harding, J. F. Hansen, O. A. Hurricane, R. P. Drake, H. F. Robey, C. C. Kuranz, B. A. Remington, M. J. Bono, M. J. Grosskopf, R. S. Gillespie

February 18, 2009

Disclaimer

This document was prepared as an account of work sponsored by an agency of the United States government. Neither the United States government nor Lawrence Livermore National Security, LLC, nor any of their employees makes any warranty, expressed or implied, or assumes any legal liability or responsibility for the accuracy, completeness, or usefulness of any information, apparatus, product, or process disclosed, or represents that its use would not infringe privately owned rights. Reference herein to any specific commercial product, process, or service by trade name, trademark, manufacturer, or otherwise does not necessarily constitute or imply its endorsement, recommendation, or favoring by the United States government or Lawrence Livermore National Security, LLC. The views and opinions of authors expressed herein do not necessarily state or reflect those of the United States government or Lawrence Livermore National Security, LLC, and shall not be used for advertising or product endorsement purposes.

Observation of a Kelvin-Helmholtz Instability in a High-Energy-Density Plasma on the Omega Laser

E.C. Harding[1], J.F. Hansen[2], O.A. Hurricane[2], R.P. Drake[1], H.F. Robey[2], C.C. Kuranz[1], B.A. Remington[2], M.J. Bono[2], M.J. Grosskopf[1], R.S. Gillespie[1]
[1]*University of Michigan, Ann Arbor, Michigan 48109*
[2]*Lawrence Livermore National Laboratory, Livermore, California 94550*

A laser initiated experiment is described in which an unstable plasma shear layer is produced by driving a blast wave along a plastic surface with sinusoidal perturbations. In response to the vorticity deposited and the shear flow established by the blast wave, the interface rolls up into large vortices characteristic of the Kelvin-Helmholtz (KH) instability. The experiment used x ray radiography to capture the first well-resolved images of KH vortices in a high-energy-density plasma, and possibly the first images of transonic shocks generated by large-scale structures in a shear layer.

The physical processes governing the evolution of a stratified fluid flow with a large velocity gradient (i.e., a shear flow) are of fundamental interest to a wide range of research areas including combustion, inertial confinement fusion (ICF), stellar supernovae, and geophysical fluid dynamics [1-4]. Traditional experiments have used inclined tanks of fluid to initiate a flow, generally at low Reynolds numbers, or wind tunnels that combine two parallel gas flows at the end of a thin wedge, known as a splitter plate. The splitter plate experiments have explored flows with maximum shear velocities on the order of 10^3 m/s and Reynolds numbers up to 10^6 [5, 6]. Here we report the creation of a novel type of shear flow, achieved by confining a laser driven blast wave in a millimeter-sized shock tube, which produced shear velocities on the order of 10^4 m/s and Reynolds numbers of 10^6 in a plasma. This system enabled the first apparent

observation of transonic shocklets, which are small, localized shocks believed to develop in response to a local supersonic flow occurring over a growing perturbation [7]. These shocklets have been predicted previously in simulations [8, 9], but have never to our knowledge been observed.

These experiments are also the first to observe the growth of perturbations by the Kelvin-Helmholtz (KH) instability under high-energy-density (HED) conditions. In all flows having steep enough shear layers, small perturbations that initially develop on an interface are amplified by KH, driven by lift forces that result from differential flow across the perturbation. As the KH instability enters its non-linear regime the growth of the perturbation begins to saturate, at which point the interaction of secondary instabilities with the primary perturbation causes the flow to transition to a fully turbulent state [10]. HED plasmas are created when an energy source, a multi-kilojoule laser in this case, creates pressures of order one Mbar or more. Such plasmas are compressible, actively ionizing, often involve strong shock waves, and have complex material properties. The one previous attempt to produce a shear flow under HED conditions was inconclusive and did not observe KH growth [11].

The KH instability and shear flow effects in general are also of practical importance in a number of HED systems. They should be considered in multi-shock implosion schemes for direct drive capsules for inertial confinement fusion (ICF), since the KH instability may accelerate the growth of a turbulent mixing layer at the interface between the ablator and solid deuterium-tritium nuclear fuel [12, 13]. Some approaches to ICF (e.g., fast

ignition [14]) produce shear flows qualitatively similar to those discussed here. Some supernova explosion models also find that KH plays an important role [15, 16]. In addition, the experiments and simulations of HED and astrophysical systems have shown that structures driven by shear flow appear on the high-density spikes produced by the Rayleigh-Taylor (RT) and Richtmyer-Meshkov (RM) instabilities [15, 17]. Both RT and RM have important consequences for the evolution of ionized, compressible flows, including those found in ICF [18] and astrophysical systems.

The shear experiments presented here were performed in rectangular, beryllium shock tubes (see Fig. 1). These shock tubes, 4.0 mm long, had interior dimensions of 1.0 mm (wide) by 2.0 mm (tall) with thicknesses of 0.200 mm and 0.500 mm on the vertical and horizontal walls, respectively. Inserted into each shock tube were two blocks of material each 1 mm tall. The upper block was carbon-resorcinol-formaldehyde (CRF) foam ($C_{1000}O_{48}H_{65}$, density $\rho = 0.100$ g/cm^3 with an average cell size of 0.02 μm) while the lower block was composed of three smaller pieces that were glued to together. The outer two of these pieces were made from polyamide/imide plastic ($C_{22}H_{14}O_4N_2$, $\rho = 1.42$ g/cm^3), each 0.40 mm wide, while the smaller, center piece was 0.20 mm wide and was made from 3% iodinated polystyrene ($C_{50}H_{47}I_3$, $\rho = 1.45$ g/cm^3). We will refer to the iodinated polystyrene piece as 'CHI' and the polyamide/imide as 'PAI'. Identical single-mode sinusoidal perturbations with wavelength $\lambda = 400$ μm and peak-to-valley amplitude = 60 μm were machined into one of the long faces of the CRF and PAI/CHI blocks. The two blocks were mated along the perturbed side and then mounted in the shock tube so that the ends were flush with the tube. One end of the shock tube was covered with a 30

μm thick polystyrene (C_8H_8, ρ = 1.05 g/cm^3) ablator. On top of the ablator was a 50 μm thick gold washer that had an outer diameter of 2.5 mm with an interior, square (1.0 x 1.0 mm) cutout that was aligned with the center of the CRF block. Attached to the front of the shock tube was a large shield that prevented the detector from being exposed to the radiation emitted from the laser-ablated plasma (see Fig. 1). The design of the shock tube components of this target is described by Hurricane [19].

The experiments were performed at the Omega laser facility at the Laboratory for Laser Energetics, University of Rochester [20]. The laser (Nd-glass, λ = 0.351 μm) delivered 4.3 ± 0.1 kJ to the target by overlapping ten "drive beams" onto the ablator, centered in the square cutout of the gold washer. Each beam had a temporal profile with 100 ps rise and fall times, a nominally flat top, and a full width at half maximum of 1.0 ns, and had an intensity profile whose shape is described by *exp[-(r / 430 μm)]$^{4.7}$*, where *r* is the distance from the center of the profile. The peak intensity of all ten overlapped beams was 8 x 10^{14} W/cm^2. The low intensity wings of the laser spot were masked by the Au washer, which prevented the disruption of the PAI/CHI blocks and the surrounding Be shock tube.

X ray radiography was used to diagnose the target evolution at t = 25, 45, and 75 ns with respect to the start of the primary laser pulse. At the specified time interval an additional three beams, each with a nominal energy of 450 J, a 1 mm diameter spot size, and a temporal pulse shape like that of the drive beams, were overlapped onto the rear of a small 200 x 200 x 5 μm vanadium foil attached to a 2 x 2 mm polystyrene substrate. The

strong laser heating of the foil generated x rays from the He-α transition (5.18 keV), which propagated through the bulk of the vanadium foil and toward the target. The x rays were apertured with a with a tapered pinhole (20 to 35 μm diameter) in a 50 μm thick tantalum substrate that was fixed 500 μm in front of the vanadium foil with the larger opening nearest to the target, and positioned 10 mm from the center of the shock tube. The vanadium x rays passed through the target, were differentially absorbed by the various target materials, and then were incident on a single piece Agfa D7 film, which was later digitized. The film was exposed for ~ 1 ns (the approximate temporal duration of the x ray emission), so motion blurring of the blast wave should be detectable given that the resolution element is between 20 and 35 μm, as set by the pinhole size. As a result of the strong absorption of He-α x rays in the CHI layer nearly all of the of the opacity of the target was concentrated in the center of the shock tube.

A time sequence of three radiographs in Fig. 2 shows the development of vortices that were initiated from the sinusoidal perturbations, and later driven to large amplitudes by the flow of CRF plasma that was created by the blast wave. The ablation of material from the polystyrene surface created a large pressure (~ 50 Mbar) that drove a strong shock into the polystyrene and then the CRF foam. When the laser drive ended a rarefaction wave was launched from the ablation surface and propagated to the shock front, which subsequently developed into a decelerating blast wave. The 2D radiation hydrodynamics code, CALE [21], predicted that the blast wave structure would form well before it entered the field of view of the diagnostic. The blast wave compressed, heated, and imparted forward momentum to the CRF foam, which led to the high-speed flow of

ionized CRF plasma. At the CRF/CHI interface the blast wave was refracted into the CHI and continued to propagate as a transmitted shock. The transmitted shock propagated in a direction nearly orthogonal to the blast wave, and in doing so was unable to impart significant forward velocity to the CHI. Consequently, vorticity was deposited at the interface and a velocity gradient developed across the interface. The resulting circulation, which is defined as the line integral of the velocity around a closed contour parallel to and centered on the interface, to first order is proportional to $Sin(\alpha)(1-\eta^{-1/2})$ where η is the density ratio of the CRF and CHI and α is the angle between the blast wave and the interface [22]. As always in KH, the shear flow and the variation in the circulation lead to the growth of structure on the interface in time. The evolution of the interface is similar to that of previous gas shock tube work, which involved oblique membranes separating gases of different densities [23-25]. However, in contrast to the present experiment, sinusoidal initial conditions were not implemented, and geometries where the shock wave and interface are orthogonal were not investigated in those experiments.

After the passage of the blast wave, CALE predicts the average ion temperature of the foam to be approximately 13 eV. The average ion temperature of the shocked CHI was approximately 0.6 eV. Although the transmitted shock does not appear in Fig. 2 due to the large opacity of the CHI, the position inferred from CALE simulations is given by the dashed lines. The rapid growth of structure on the interface did not appear in CALE simulations without imposed perturbations.

We estimated the linear-theory KH growth rate for the interface perturbations after they were compressed by the blast wave. The perturbation directly behind the blast wave in Fig. 2 (a) was compressed to a peak-to-valley height of 44 μm while the wavelength was decreased to approximately 200 μm. The blast wave traveled ~ 1.5 mm from its origin at the front of the ablator in 25 ns with an average speed of 60 μm/ns. In Fig. 2 (a) the leading edge of the blast wave appeared to be blurred over 150 μm due to a combination of an oblique line of sight and curvature of the blast wave across the width of the shock tube. In Fig. 2 (a) the CRF density, measured from the x ray absorption, near the perturbations at x = 1.0 mm and y = - 0.5 mm was 0.38 g/cm^3 and closer to the interface at x = 1.0 mm and y = -0.2 mm the density was 0.28 g/cm^3. The maximum measured density in the CRF behind the blast wave in Fig. 2(a) was ~ 0.42 g/cm^3, which was 4.2 times the pre-shock density. By requiring the conservation of mass flux across the blast wave we find that CRF plasma immediately behind the blast wave had a speed of ~ 45 μm/ns. However, as expected, the flow behind the blast wave was unsteady, with the velocity decreasing monotonically in the downstream direction. During the period from the passage of the blast wave to t = 45 ns the left-most perturbation in Fig. 2 experienced an average velocity difference of 18 μm/ns. The KH incompressible linear growth rate for an infinitely sharp interface with a horizontal velocity difference of ΔU is equal to $k \Delta U \sqrt{(\rho_{CRF} \rho_{CHI})}/(\rho_{CRF} + \rho_{CHI})$, where ρ_{CRF} and ρ_{CHI} are the densities of the shocked CRF and CHI and k is the perturbation wave number. Using the density measured near the perturbations we have $\rho_{CRF} = 0.38$ g/cm^3, and assuming the CHI was compressed by a factor of 2, as indicated by CALE, we have $\rho_{CHI} = 2.9$ g/cm^3. Taking $k = 2\pi/200$ μm and

$\Delta U = 18$ μm/ns gives 5.5 ns as an e-fold time, implying an average, linear rate of increase of the amplitude of ~ 11 μm/ns.

Fig. 3 shows the height of the perturbation as a function of the time elapsed, t_e, since the leading edge of the blast wave was centered on the crest of the perturbation. The blast wave timing, inferred from CALE simulations, was systemically adjusted by 5 ns so that the location of the blast wave in the simulation matches that of the experiment at t = 25 ns. Immediately after the blast wave passes the crest of a perturbation mass appeared to be stripped in a process perhaps similar to that described by Hansen et. al. [26]. After compression, the average perturbation growth speed was ~ 4 μm/ns; the data suggest faster growth before t_e = 30 ns and slower growth after. Reflected waves are seen emanating from the perturbation behind the blast wave in Fig. 2 (a) and the right most perturbation in Fig. 2 (b). In Fig. 2(c) the structure seen in the cores appears to dissolve in the older roll-ups, which may indicate a transition to turbulence. The Reynolds numbers for the CRF and CHI, for the conditions of the left-most perturbation in Fig. 2 (b) ($\Delta U = 5$ μm/ns, L = 180 μm, $\nu_{CRF} = 0.30$ cm^2/s, and $\nu_{CHI} = 0.002$ cm^2/s) are 3x10^4 and 5x10^6, respectively, using published viscosity formulae [27] and parameters from the CALE simulations. Ultimately if the flow were to go fully turbulent, the roll-ups would be accompanied by a 3D secondary instability that materializes as small counter-rotating streamwise vortices on the outside of the main roll-ups [6]. Yet, these streamwise vortices are typically an order of magnitude smaller than the primary roll-up [28] and therefore not resolvable with our current diagnostic.

We believe that the bright bubbles that are visible on the downstream side of the left-most roll-up in Fig. 2 (b) and the two-left most roll-ups in Fig. 2 (c) are transonic shocklets. They are relatively bright in the radiograph, which implies that they are regions of lower density. When subsonic CRF flow is forced around the roll-ups (as viewed in the frame of reference moving with the vortices) and becomes supersonic, the density will decrease in response. Using the local sound speed and flow speed taken from CALE simulations at t = 45 ns and at the location (x = 1.0 mm, y = -0.4 mm) the Mach number was estimated to be 0.15, which supports the idea that the flow maybe only locally supersonic. Furthermore, three-dimensional effects have been ruled out as a possible explanation due to the well defined structure of the shocklets despite the fact that the radiograph has been integrated over the entire 1 mm width of the CRF foam. By comparing the sizes of the shocklets in Fig. 2 (c) we estimate the shocklets are expanding at ~14 μm/ns. Shocklets have not appeared in high-resolution 2D CALE simulations, and this is the first time they have been observed in any HED plasma experiment. Moreover, their existence in other numerical simulations has been predicted [8, 9] but to our knowledge never experimentally observed anywhere.

In conclusion, this experiment is significant because it demonstrates a novel method for creating a shear flow and is the first to create a diagnosable KH instability in a HED system. Future laser-driven experiments, using steady shocks rather than blast waves, could push the Reynolds number above 10^7. Understanding the KH instability is important because it plays a central role in the transition to turbulence in many HED, astrophysical, and other fluid systems. We also believe we have observe the first

transonic shocklets in a shear flow experiment. Currently, simulations are unable to

reproduce these shocklets, indicating that this type of shear flow experiment provides a

rigorous test for bench-marking numerical simulations.

[1]   S. A. Thorpe, J. Geophys. Res.-Oceans **92**, 5231 (1987).
[2]   K. C. Schadow, and E. Gutmark, AIAA Pap. 89-2786 (1989).
[3]   M. H. Emery, J. H. Gardner, and J. P. Boris, Phys. Rev. Lett. **48**, 677 (1982).
[4]   R. A. Chevalier, J. M. Blondin, and R. T. Emmering, Astrophys. J. **392**, 118 (1992).
[5]   D. Papamoschou, and A. Roshko, J. Fluid Mech. **197**, 453 (1988).
[6]   G. L. Brown, and A. Roshko, J. Fluid Mech. **64**, 775 (1974).
[7]   P. E. Dimotakis, in *Progress in Astronautics and Aeronautics*, edited by S. N. B. Murthy, and E. T. Curran (AIAA, Washington, DC, 1991), pp. 265.
[8]   S. K. Lele, AIAA 27th Aerospace Sciences Meeting, Paper 89-0374 (1989).
[9]   D. Vandromme, and H. Haminh, *Turbulence and Coherent Structures* (Kluwer AP, Dordrecht, 1989).
[10]   C. P. Caulfield, and W. R. Peltier, J. Fluid Mech. **413**, 1 (2000).
[11]   B. A. Hammel *et al.*, Phys. Plasmas **1**, 1662 (1994).
[12]   K. O. Mikaelian, Phys. Fluids **6**, 1943 (1994).
[13]   P. Diamond *et al.*, in *JASON Report No. JSR-91-325* (MITRE Corporation, 1993).
[14]   M. Roth *et al.*, Phys. Rev. Lett. **86**, 436 (2001).
[15]   K. Kifonidis *et al.*, Astron. Astrophys. **408**, 621 (2003).
[16]   J. C. Wheeler, J. R. Maund, and S. M. Couch, Astrophys. J. **677**, 1091 (2008).
[17]   A. R. Miles *et al.*, Phys. Plasmas **11**, 3631 (2004).
[18]   S. Atzeni, and J. Meyer-ter-Vehn, *The physics of inertial fusion : beam plasma interaction, hydrodynamics, hot dense matter* (Oxford University Press, Oxford, 2004), pp. xxii.
[19]   O. A. Hurricane, High Energy Density Physics **4**, 97 (2008).
[20]   T. R. Boehly *et al.*, Opt. Commun. **133**, 495 (1997).

[21]   R. T. Barton, in Numerical astrophysics : proceedings of a symposium in honor of James R. Wilson, held at the University of Illinois in October, 1982, edited by J. M. Centrella *et al.* (Jones and Bartlett Publishers, University of Ilinois, 1982).
[22]   R. Samtaney, and N. J. Zabusky, J. Fluid Mech. **269**, 45 (1994).
[23]   R. G. Jahn, J. Fluid Mech. **1**, 457 (1956).
[24]   A. M. Abdelfattah, and L. F. Henderson, J. Fluid Mech. **86**, 15 (1978).
[25]   L. F. Henderson, J. Fluid Mech. **26**, 607 (1966).
[26]   J. F. Hansen *et al.*, Phys. Plasmas **14**, 12 (2007).
[27]   J. G. Clerouin, M. H. Cherfi, and G. Zerah, Europhys. Lett. **42**, 37 (1998).
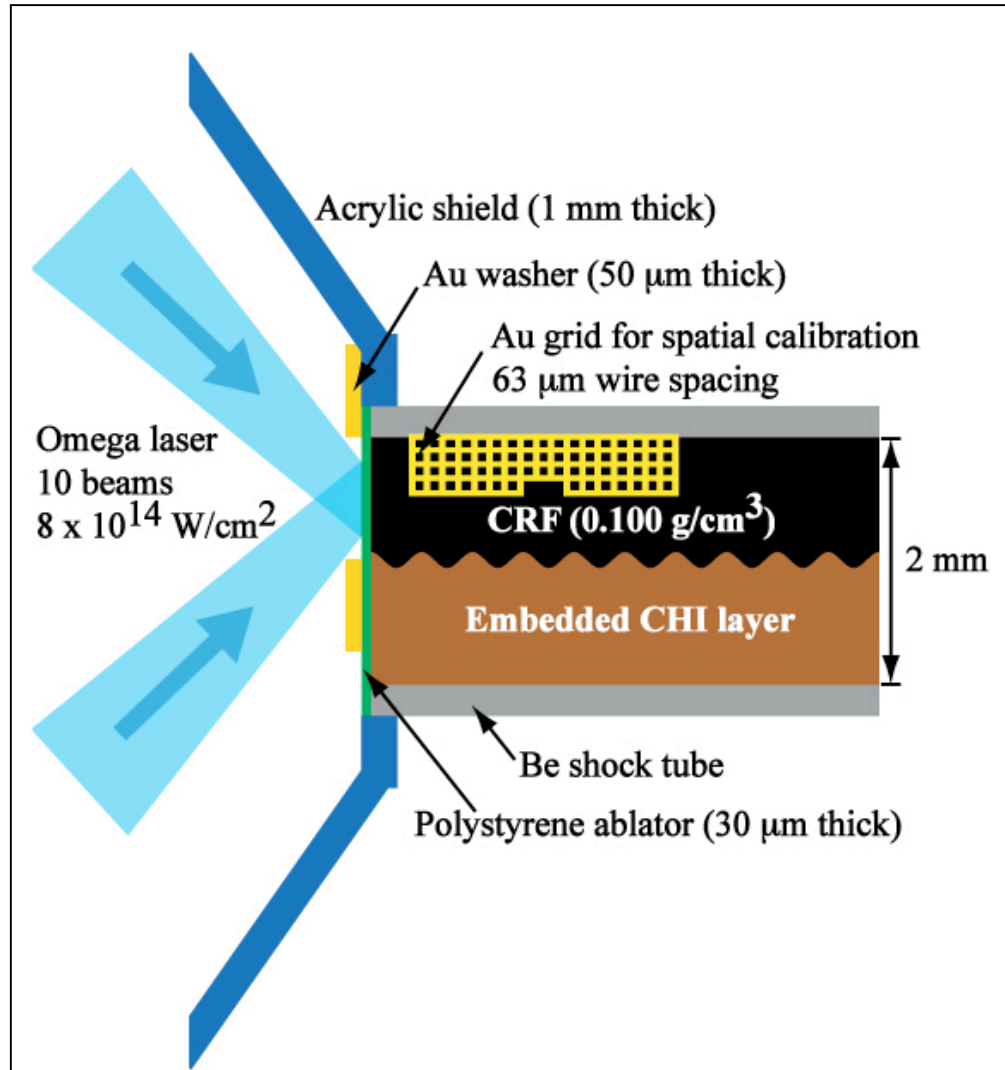[28]   W. R. Peltier, and C. P. Caulfield, Annu. Rev. Fluid Mech. **35**, 135 (2003).

FIG. 1. A cross-sectional view of the Kelvin-Helmholtz target. The sinusoidal perturbation had a wavelength of 400 μm and a peak-to-valley amplitude of 60 μm. The Au grid was attached to the outside of the shock tube, but it is shown here for clarity.
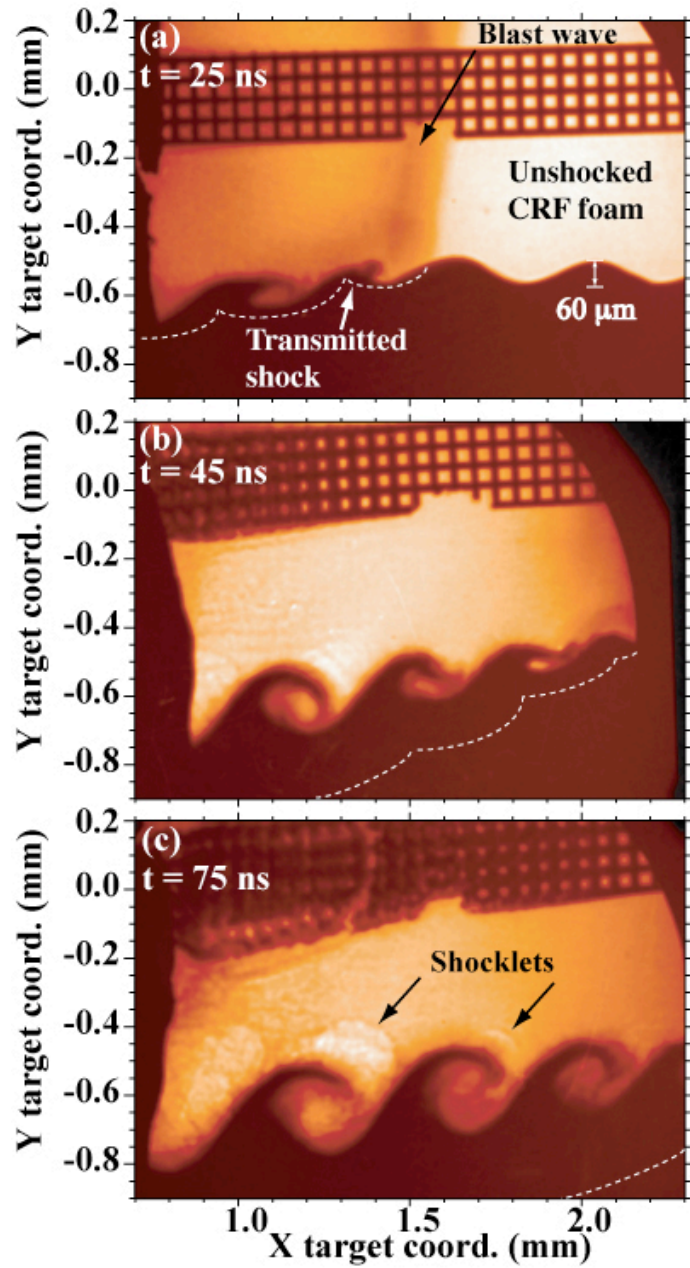
FIG. 2. X-ray radiographs of three identical targets that show the formation of large Kelvin-Helmholtz roll-ups. These radiographs were captured at 25 ns (a), 45 ns (b), and 75 ns (c) after the start of the drive beam pulse. The dotted line shows the location of the transmitted shock inferred from CALE simulations. Here the origin of the x and y-axes was defined by the nominal position of the drive beams on the polystyrene ablator. The placement of the axes on the images is accurate to within 10%. The Au grid was distorted by the blast wave when it broke out from the inside of the shock tube and struck the grid. These images are displayed with no post processing.
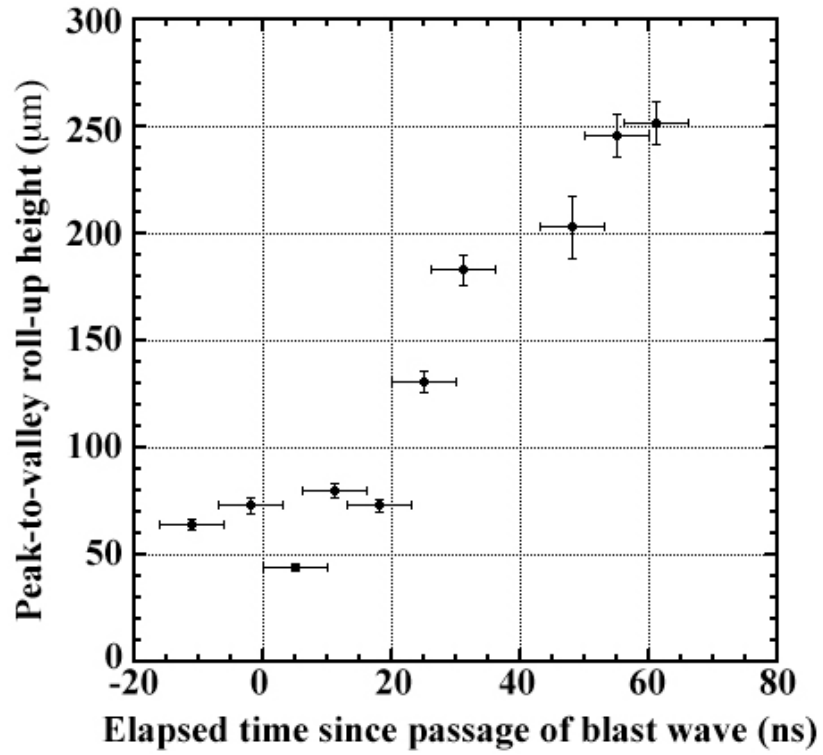
FIG. 3. Experimental measurements of the peak-to-valley KH roll-up heights observed over multiple targets. The perturbations are first compressed and then increase in size until they appear to saturate. The elapsed time was inferred from CALE simulations and then systematically adjusted based on the experimental blast wave location seen at t = 25 ns in FIG. 2.